Atmos. Chem. Phys. Discuss., 11, 27661–27699, 2011
www.atmos-chem-phys-discuss.net/11/27661/2011/
doi:10.5194/acpd-11-27661-2011

Atmospheric Chemistry and Physics Discussions

Aerosol chemical composition at Cabauw, the Netherlands as observed in two intensive periods in May 2008 and March 2009

A. A. Mensah[1,*], R. Holzinger[2], R. Otjes[3], A. Trimborn[1], T. F. Mentel[1], H. ten Brink[3], B. Henzing[4], and A. Kiendler-Scharr[1]

[1]Institut für Energie- und Klimaforschung: Troposphäre (IEK 8), Forschungszentrum Jülich GmbH, Jülich, Germany
[2]Institute for Marine and Atmospheric research Utrecht (IMAU), Utrecht, The Netherlands
[3]Energy research Centre of the Netherlands (ECN), Petten, The Netherlands
[4]Netherlands Organisation for Applied Scientific Research (TNO), Utrecht, The Netherlands
[*]now at: Institute of Atmospheric and Climate Science (IAC), ETH Zurich, Zurich, Switzerland

Received: 5 September 2011 – Accepted: 28 September 2011 – Published: 12 October 2011

Correspondence to: A. A. Mensah (amewu.mensah@env.ethz.ch)

Published by Copernicus Publications on behalf of the European Geosciences Union.

Abstract

Observations of aerosol chemical composition in Cabauw, the Netherlands, are presented for two intensive measurement periods in May 2008 and March 2009. Submicron aerosol chemical composition was measured by an Aerodyne Aerosol Mass Spectrometer (AMS) and is compared to observations from aerosol size distribution measurements as well as composition measurements with a Monitor for AeRosol and GAses (MARGA) based instrument and a Thermal-desorption Proton-transfer-reaction Mass-spectrometer (TD-PTR-MS). An overview of the data is presented and the data quality is discussed. In May 2008 enhanced pollution was observed with organics contributing 40 % to the PM_1 mass. In contrast the observed average mass loading was lower in March 2009 and a dominance of ammonium nitrate (42 %) was observed. The semi-volatile nature of ammonium nitrate is evidenced in the diurnal cycles with maximum concentrations observed in the morning hours in May 2008 and little diurnal variation observed in March 2009. Size dependent composition data from AMS measurements are presented and show a dominance of organics in the size range below 200 nm.

1 Introduction

Aerosol particles directly and indirectly affect the global climate. Depending on their optical properties, particles can scatter or absorb long and short wave radiation. This can have cooling or heating effects on the atmosphere and has thus a direct impact on the radiation balance of the Earth (e.g. global dimming, Nazarenko and Menon, 2005; Ramanathan et al., 2007; Romanou et al., 2007). Aerosol particles also exhibit a range of indirect effects in acting as cloud condensation nuclei (CCN). Changes in particle number concentration and size distribution alter cloud albedo (Norris and Wild, 2007) and can cause suppression or enhancement of rain (Nober et al., 2003; Tao et al., 2007; Phillips et al., 2002). The IPCC report 2007 identifies aerosol particles as the major

ACPD
11, 27661–27699, 2011

uncertainty in the prediction of future climatic conditions (IPCC, 2007). Aerosol particles are providing the surface for heterogeneous reactions, thus affect the atmospheric lifetime of atmospheric trace constituents (Dentener and Crutzen, 1993). Furthermore, aerosol particles control the visibility and are associated with health hazards such as increased cardiopulmonary (Moolgavkar et al., 1994) or lung cancer mortality (Pope et al., 2002). Apart from water, the major constituents found in atmospheric aerosol particles are sulfate, nitrate, ammonium, minerals, black carbon (BC) and organic components often referred to as organic matter (OM) (Rogge et al., 1993). The fractional abundance of the individual constituents is strongly dependent on the particles origin and processing during their atmospheric lifetime.

Ammonium nitrate is a major component of the PM_1 mass in polluted regions of Europe where reductions in sulfur dioxide emissions have reduced the occurrence of ammonium sulfate (Monks et al., 2009). Also the ubiquity of organic components in boundary layer aerosol particles is well documented (Zhang et al., 2007). Recently Jimenez et al. (2009) pointed out that atmospheric aging lowers the organic aerosol volatility and thus enhances the persistence of the particulate organic aerosol fraction and their hygroscopic properties (Jimenez et al., 2009; Morgan et al., 2010b).

Here we present an overview of the aerosol composition as measured in two intensive observation periods at Cabauw, the Netherlands. The measurements were linked to the intensive observation periods of the European Integrated Project on Aerosol Cloud Climate and Air Quality interactions (EUCAARI) (Kulmala et al., 2009) and activities of the European Monitoring and Evaluation Programme (EMEP, http://www.emep.int/). Previous work on this data set has focused on the aerosol direct effect (Roelofs et al., 2010; Morgan et al., 2010a) and showed that the high fraction of ammonium nitrate observed in May 2008 largely impacts the aerosol optical thickness (Roelofs et al., 2010). It was shown that due to its semi-volatile nature maximum concentrations of ammonium nitrate are observed at the top of the boundary layer (Morgan et al., 2010a). The height profile needs to be taken into account when modeling the aerosol direct effects. Here we focus on the comparison of different instruments that

ACPD
11, 27661–27699, 2011

measured the inorganic aerosol components in May 2008. Aerosol particle mass spectrometric data is compared to the results obtained by MARGA and Thermal-Desorption Proton-Transfer-Reaction Mass-Spectrometry (TD-PTR-MS) measurements. We show that the inorganic particulate aerosol mass concentrations derived by the different approaches are in good agreement with each other. Diurnal patterns of inorganic and organic aerosol are discussed and an overview of the concentrations observed in the two campaigns is presented.

2 Experimental

2.1 CESAR tower

As part of EMEP and the EUCAARI project, several intensive observations periods were defined during which the aerosol particles chemical composition was characterized by aerosol mass spectrometry (AMS) at a number of field sites throughout Europe (Kulmala et al., 2011). An Aerodyne High Resolution Time of Flight AMS (HR-ToF AMS, hereafter referred to as AMS) was operated at the Cabauw Experimental Site for Atmospheric Research (CESAR), The Netherlands, during two of these intensive observation periods. The first campaign (Intensive Measurement Period At Cabauw Tower, IMPACT) took place in May 2008, the second in March 2009. The CESAR observatory (51° 57′ N, 4° 54′ E, −0.7 m a.s.l.) is located at a rural site in the center of the Netherlands, about 20 km south-west of Utrecht and 50 km south of Amsterdam. The measurement site is representative for North-West Europe and features continental and maritime conditions, depending on the wind direction. The plain geography of the Netherlands and especially in the area of Cabauw reduces ambiguities in terms of air parcel convection and turbulences. The CESAR observatory is run by the Royal Netherlands Meteorological Institute (KNMI), De Bilt, The Netherlands. The site features a 213 m high tower equipped with standard measurement devices for outside and dew point temperature, and wind direction and speed at 200 m, 140 m, 80 m, 40 m,

ACPD
11, 27661–27699, 2011

20 m, 10 m, and 2 m height. Beside this, precipitation, cloud cover and height, radiation and a range of remote sensing, flux and concentration measurements of Green House Gases (GHG) are continuously performed (Russchenberg et al., 2005).

2.2 AMS

The AMS was located in the tower basement, sampling from an aerosol sampling line, which was shared with other aerosol instrumentation. The inlet system consisted of four parts: (a) 4 PM_{10} size selective inlets, (b) a Nafion drying system that dried the aerosol stream to or below 40 % relative humidity, (c) a 60 m stainless steel pipe, and (d) a manifold that splits the flow to a variable suite of instruments. Instruments sampled their flow from the manifold using separate pumps to adjust the required flow for proper operation. The total flow sustained in the 60 m inlet pipe was kept at about 60 l min^{-1}, which was the highest flow that warranted laminar flow ($Re \approx 2000$). Excess air was drawn through the sampling heads and the pipe to assure optimal operation of the PM_{10} inlets and to keep the flow in the pipe at 60 l min^{-1} even if the suit of instruments used less. Whenever an instrument was added or removed from the manifold, the excess air and flows to the other instruments were checked and adjusted when needed. The entire distance between tower inlet at 60 m height and AMS inlet was about 70 m. The AMS was connected to the sampling manifold by 3 m stainless steel tubing with an inner diameter of 4 mm. The flow of 680 ml min^{-1} between the manifold and the AMS inlet was achieved by parallel sampling of the AMS (80 ml min^{-1}) and an Ultrafine Condensational Particle Counter (UCPC, TSI 3786, 600 ml min^{-1}).

The working principles of the Aerodyne Aerosol Mass Spectrometer AMS were described in detail elsewhere (Canagaratna et al., 2007; Jayne et al., 2000; Jimenez et al., 2003). A brief summary of the modes of operation and calibrations performed during the campaigns follows here.

The AMS allows the mass spectrometric online investigation of aerosol particle composition after substantial reduction of the gas phase. The AMS can be separated into four sections: an aerodynamic lens as inlet, a differentially pumped vacuum particle

ACPD
11, 27661–27699, 2011

sizing chamber, a vaporization/ionization region and a mass spectrometer (MS). An aerosol stream of 80 ml min^{-1} passes through a Liu type aerodynamic lens (Liu et al., 1995a,b). The lens reduces the gas phase to particle phase concentration by a factor of 10^7. This gas phase reduction is a key feature since gaseous nitrogen alone has a concentration of 950×10^6 µg m^{-3} in the air and particulate aerosol concentrations range from a few micrograms per meters cubed in remote areas like Hyytiälä, FI (Zhang et al., 2007) to about 100 µg m^{-3} in polluted areas like Mexico City, MX (Aiken et al., 2009). The lens has an almost 100 % transmission efficiency for particles between 70 nm and 500 nm. Particles in the size ranges of 30 nm to 70 nm and 500 nm to 2500 nm are still substantially transmitted, with a 50 % transmission efficiency for particles of 1 µm (Jayne et al., 2000; Zhang et al., 2004). Hence, the AMS is referred to as PM_1 instrument (Canagaratna et al., 2007). The particle sizing is achieved in a differentially pumped particle sizing chamber by measuring the particles time of flight (PToF) between entering the chamber and detection. After passing through the PToF chamber the particle beam strikes the vaporizer. In general, the vaporizer is operated at approximately 600 °C causing the non-refractory components of the particles to flash evaporate on the surface (Jayne et al., 2000). The evaporated molecules are ionized by 70 eV electron impact (EI) and are then extracted into the MS for compositional analysis. The HR-ToF mass spectrometer acquires a full mass spectrum in one ion extraction, which occurs every 30 µs in V-mode and every 50 µs in W-mode. V- and W-mode refer to the flight path of the ions within the MS. V-mode is a single reflection flight path (1.3 m) and W-mode is a triple reflection flight path (2.9 m) with resolving powers of about 2000 and 4000, respectively (DeCarlo et al., 2006). This allows for a clear separation of different ions of the same nominal mass such as $C_2H_3O^+$ and $C_3H_7^+$ on *m/z* 43. In the so called MS mode of operation mass spectral information is collected over the integral aerosol size distribution. In the PToF mode of operation size dependent compositional data is acquired.

For quantitative measurements with the AMS the ionization efficiency (IE) needs to be determined by a calibration with ammonium nitrate particles (Drewnick et al., 2004;

ACPD
11, 27661–27699, 2011

Jayne et al., 2000). In the standard calibration procedure as performed here dried and size selected ammonium nitrate particles are measured with the AMS and a condensational particle counter (CPC) in parallel. Taking the bulk density of ammonium nitrate, the size, and the number of the particles, the total mass of aerosol particles introduced into the AMS is calculated. This value is compared to the detected ion signal of the mass spectrometer. A scaling factor is introduced to link the amount of molecules introduced into the AMS with the ion count per molecule detected by the AMS. The scaling factor, the so called IE, is in general at the order of 10^{-6} ions/molecule. The ammonium nitrate calibration allows for the determination of other aerosol compounds in terms of nitrate equivalent mass. The actual mass of the compound of interest can be determined, when the compounds specific ionization efficiency is known. In practice, ionization efficiencies relative to the ionization efficiency of nitrate (IE_{NO_3}) are used. These ionization efficiencies are called relative ionization efficiencies (RIE). E.g., the RIE of ammonium (RIE_{NH_4}), which is determined during the standard IE calibration, is generally about 4.

Another quantity that needs to be determined for quantitative measurements with the AMS is the Collection Efficiency (CE, Huffman et al., 2005). The CE is a unit less quantity, which accounts for the difference between aerosol mass entering the instrument and the detected mass. Dry and solid particles, e.g. particles with a high sulfate mass fraction, tend to bounce off the vaporizer without being evaporated i.e., substantial amounts of the introduced particulate mass will not be detected in the MS. That means in reverse, the ratio of introduced to detected amount is favored for wet or waxy particles, e.g. particles with a high nitrate mass fraction. The CE determination will be explained in detail in an upcoming section.

In both observation periods, the aerosol stream was dried by two Nafion dryers at the inlet at 60 m height. Therefore, RH values measured in the sampling line do not reflect ambient RH. The RH time series were incorporated into the AMS data analysis to apply a time dependent correction for the contribution of gas phase water (RH) to the total water signal detected by the AMS. A relative ionization efficiency of water

ACPD
11, 27661–27699, 2011

(RIE_{H_2O}) of 2 as determined by Mensah et al. (2011) was applied for determinations of the residual particulate water. Size calibrations were performed through measurements of the particle time of flight of polystyrene latex particles (PSL, Duke Scientific Corporation, Palo Alto CA) of defined sizes.

At Cabauw, the AMS was operated in alternation mode, switching between V-mode (MS, and PToF mode) and W-mode (MS mode only) regularly. The vaporizer temperature was set to about 580 °C throughout both sampling periods. The AMS was run on remote control to enable permanent control of the instrument performance. Particle size and ionization efficiency calibrations were performed once a week. Regular measurements with a High Efficiency Particulate Air (HEPA) filter in line were performed to determine the gas phase background signal. Data was collected with a time resolution of 5 min.

The data acquired with the AMS will be compared to data acquired by several other collocated aerosol measurement instruments. In the following short descriptions of a Scanning Mobility Particle Sizer (SMPS, TSI 3034), two Monitor for AeRosol and GAses (MARGA, ten Brink et al., 2007) instruments, and a Thermal-Desorption Proton-Transfer-Reaction Mass-Spectrometer (TD-PTR-MS, Holzinger et al., 2010b) will be given.

2.3 SMPS

Likewise the AMS, the SMPS was located in the basement and sampled from the common aerosol inlet line. It was operated with 5 min time resolution and the particle number size distributions covering the diameter range from about 10 nm to 470 nm were measured with a log-equidistant resolution of 32 size bins per decade in both campaigns.

ACPD
11, 27661–27699, 2011

2.4 MARGA

The two MARGA instruments sampled at a separate inlet at 4 m height and collected aerosol at ambient RH and temperature. The MARGA is a combination of a Wet Annular Denuder (WAD) followed by a Steam Jet Aerosol Collector (SJAC, Slanina et al., 2001) to facilitate the chemical online analysis of water soluble gases and particulate aerosol components at the same time (Trebs et al., 2004). The instrument can be run with different inlets to confine the particle size range. The MARGA-2S was deployed as the standard Applikon instrument (http://misp.metrohm.com/gaseous/MARGA_catalogue.html). The MARGA-2S was in operation at the Cabauw site as part of the Dutch Beleid Ondersteunend Project (BOP) program for over a year (September 2007–October 2008). It measured both the PM_{10} and $PM_{2.5}$ fraction. This was accomplished by sampling the ambient air with a Teflon coated PM_{10} impactor at 2 $m^3\,h^{-1}$. A polyethene tube carried the sample air to an indoor splitter. The outdoor length of 2 m was surrounded by a fan driven outdoor airflow to prevent wall interactions. Indoors, the sample lines were insulated for the same purpose. After the iso-kinetic split the two lines were connected to the two MARGA sampling boxes. In one of the lines a Teflon coated $PM_{2.5}$ cyclone was inserted. The Marga-2S was serviced on a weekly basis. Both sample flows were calibrated. The analytical part, the anion and cation ion chromatography (IC), was continuously calibrated by a traceable internal LiBr standard solution. Generally the sum of the PM_{10} ions represents 50 % of the PM_{10} mass fraction. The measured ion concentrations compared well with filter measurements (Schaap et al., 2010).

The MARGA-Sizer (ten Brink et al., 2007) was located beside the MARGA-2S and sampled through the same inlet. It was operated throughout the year 2008 as part of the Dutch Besluit Subsidies Investeringen Kennisinfrastructuur BSIK program. The MARGA-Sizer sampled ambient air through a 1 $m^3\,h^{-1}$ Teflon coated $PM_{2.5}$ impactor at 30 l min^{-1}, which represents about the particle fraction with diameters smaller than 2 µm. The outdoor inlet was surrounded by the same outdoor airflow as used for

ACPD
11, 27661–27699, 2011

the MARGA-2S. Key difference between the MARGA-2S and MARGA-Sizer is a pre-separator of parallel mounted impactors for size classification defining the measurement range of the particles by different cut off sizes. During May 2008 the MARGA-Sizer was operated with 5 Moudi impactor stages of the following cut off sizes: 0.18 µm, 0.32 µm, 0.56 µm, 1.00 µm, and 2.00 µm. The cut off characteristics of the Moudi stages were checked with mono disperse Latex spheres prior to the May 2008 IMPACT campaign. Additionally to the five impactor inlets, an inlet equipped with a particle filter was used to perform blank measurements and determine the background concentration of the compounds. Measurements through the different size classes were alternated, resulting in a semi-continuous measurement but gaining insights to the size distribution of the individual species. In the standard 2 h cycle the blank was analyzed twice, while each impactor stage, the direct connection and the denuder (gas phase measurements) only once. The time coverage per fraction was thus 12.5 %. Due the low concentrations in the sample solutions for the smallest fractions the ICs were equipped with concentrator columns instead of the standard injection loops. Calibration and servicing of the MARGA-Sizer was the same as for the MARGA-2S. The MARGA-Sizer output was normalized by a factor 1.8 to match with the MARGA-2S results. The cause of deviation remained unexplained and implications will be discussed below.

2.5 TD-PTR-MS

The TD-PTR-MS instrument was located inside the building next to the MARGA instruments. Aerosol was sampled from the roof at a height of 5 m above the ground through a 10 m long non-insulated copper tube with an inner diameter of 4 mm. The system consists of a modified commercial PTR-MS (Ionicon Inc., Innsbruck, Austria, Hansel et al., 1995; Lindinger et al., 1998) which is equipped with both a gas and an aerosol inlet. Since detailed descriptions can be found in Holzinger et al. (2010a) and Holzinger et al. (2010b) only a brief description follows. The centerpiece of the aerosol inlet is a Collection-Thermal-Desorption (CTD) cell (Williams et al., 2006, Aerosol Dynamics, Berkeley, CA, USA), which collects ambient particles in the 0.07 µm to 2.00 µm size

ACPD
11, 27661–27699, 2011

range at an air sample flow rate of 1 l min^{-1}, and allows for gradual thermal desorption of the collected sample into the PTR-MS system. Particle collection is achieved by humidification-aided impaction onto the stainless steel collection surface using a sonic jet impactor. Humidification was needed to reduce particle rebound. Additionally, the CTD cell contains an auxiliary injection port for the manual introduction of liquid standards by means of a syringe. The transfer lines and the PTR-MS drift tube were operated at elevated temperatures of 200 °C to avoid re-condensation of evaporated particulate aerosol compounds. A measurement cycle of the TD-PTR-MS system is as follows: while the PTR-MS is connected to the gas phase inlet, ambient air is pulled through the CTD cell and the aerosol particles are collected on a sharp point in the CTD cell. Due to the high operating temperature of the PTR-MS drift tube and inlet lines a significant fraction of the aerosol particles evaporate, so that in the gas-phase channel the combined signal of gas phase and condensed-phase organics is detected. After aerosol collection a small flow of 10 ml min^{-1} to 12 ml min^{-1} of nitrogen carrier gas transports 100 % of the compounds evaporating from the CTD cell directly into the PTR-MS. The temperature of the CTD cell is ramped from ambient temperatures to 350 °C, which takes about 15 min at a ramping rate of 25 °C min^{-1}. After a cool down period of 10 min to 15 min a new collection cycle can be started. The operation including valve switching and heating/cooling is automated and therefore the system is capable of continuous measurements over extended periods of time.

The instrument was equipped with a quadrupole mass filter which recorded full mass spectra in the mass range of 20 Da to 219 Da at a scanning speed of 0.2 s mass unit^{-1}, so a full mass scan was completed every 40 s. The TD-PTR-MS detects all species with the same sensitivity and signals of the measured aerosol species can be directly related to a mass concentration without calibration. While Holzinger et al. (2010a) pointed out that in principle all desorbable organic aerosol compounds should be detectable with this method, reservations hold with respect to possible fragmentation during proton transfer or thermal dissociation on the CTD cell which can produce simple structures such as CO_2, CO or NO_2 that are not detected by PTR-MS. If not otherwise

ACPD
11, 27661–27699, 2011

mentioned, concentrations of individual aerosol species have been calculated according to the procedure outlined in Holzinger et al. (2010b).

3 Results and discussion

3.1 Measurement conditions

The aerosol composition as observed with the AMS is shown in Fig. 1. The top graph (Fig. 1a) presents data from May 2008 and the bottom graph (Fig. 1b) data from March 2009. The most upper panels in both graphs show the wind direction. As a guidance of the eye, northerly wind directions are colored in blue, southerlies in red, and easterly and westerly wind directions in green. Ambient temperature (T) and the relative humidity (RH) at 40 m height are given in the second upper panel. Particle mass loadings of organics (Org, green), nitrate (NO_3, blue), sulfate (SO_4, red), ammonium (NH_4, orange), and chloride (Cl, pink) are shown in the second lowest panels, as well as the total non-refractory mass loading (black), i.e. the sum of these species. The contributions of the individual species to the total mass are shown as a function of time in the bottom panels of Fig. 1a and b. Gaps in the time series are due to instrument failure, instrument maintenance, calibrations, or filter measurements.

The 2008 measurement period was dominated by easterly and south-easterly wind directions (top panel in Fig. 1a) transporting air masses from Eastern and Central Europe to the measurement site. An overview of the synoptic situation over Europe through the campaign is given by Hamburger et al. (2011). From 17–20 May northerly winds from the North Sea prevailed, transporting low mass loadings of aerosol particles ($< 5\,\mu g\,m^{-3}$) due to precipitation scavenging. This time period is referred to as scavenged background situation from here on. Though not reflected in the local wind profile, the meteorological background was dominated by long range transport of Sahara dust from North Africa from 23 May on (Roelofs et al., 2010), from here on referred to as Sahara dust period. The particulate aerosol mass loading reached maximum

ACPD
11, 27661–27699, 2011

concentrations of more than 30 µg m^{-3} during this period. As opposed to 2008, the measurement period in 2009 was dominated by westerly winds (top panel in Fig. 1b), almost uniformly covering the entire range from South to North. Only on 29 February and in the period from 17 March 2009 to 21 March 2009 easterly winds, predominantly from north-easterly directions, were present.

As mentioned above, the aerosol stream was dried by two Nafion driers in both campaigns. Since the temperatures in the basement were generally higher than the ambient temperature, the positive temperature gradient caused a further reduction of the RH within the sampling line. In May 2008, the ambient temperature and RH ranged from 6.5 °C to 25.2 °C and 24.5 % to 99.8 %, respectively, with average values of 15.5 °C and 62.8 %, respectively. In the same time period, the temperature at the AMS inlet ranged from 22.7 °C to 29.4 °C with an average of 26.5 °C and the RH ranged from 12.7 % to 42.2 % with an average of 23.1 %. This indicates, that the temperature was generally higher and the RH lower in the basement accompanied by a considerably reduced spread in the values. Since the measurement period in 2009 took place in early spring, recorded temperatures were lower and RH higher compared to the summer campaign in 2008. In March 2009, the average ambient temperature was only 7.0 °C ($0.7 \leq T$ [°C] ≥ 11.2) and the average RH as high as 77.6 % ($31.9 \leq$ RH [%] ≥ 99.2). As opposed to 2008, RH and temperature data were not available at the AMS inlet, but the average temperature and RH measured at 60 m height with in the sampling line was 18.5 °C ($16.5 \leq T$ [°C] ≥ 22.4) and 37.3 % ($23.2 \leq$ RH [%] ≥ 57.4), respectively. As already mentioned in the experimental section, beside the RIE_{H_2O}, the RH in the basement in 2008 and in the pipe in 2009, respectively, was taken into consideration in data analysis to calculate the residual particulate water content detected by the AMS. The average residual particulate water was 0.64 µg m^{-3} in 2008 and 0.31 µg m^{-3} in 2009 corresponding to 6.6 % and 5.5 % of the average particulate mass reported for 2008 and 2009, respectively.

ACPD
11, 27661–27699, 2011

3.2 Aerosol particle composition

The temporal evolution of the total particle mass loading as well as the individual species as shown in the middle panel in Fig. 1a resulted in an average mass loading of 9.72 $\mu g\,m^{-3}$ in spring 2008. The chemical composition of the aerosol particles was generally dominated by organics (bottom panel in Fig. 1a), accounting for 40 % of the total mass averaged over the measurement period (Fig. 2a). The second dominant contributor to the particles composition was nitrate (26 %), which was distinctly anti-correlated to sulfate (18 %). The scavenged background situation during mid of May was characterized by an average mass loading of only 3.56 $\mu g\,m^{-3}$ accompanied by a high fractional abundance of sulfate and a very low fractional abundance of nitrate. In contrast to that, the Sahara dust period had an average mass loading of 13.80 $\mu g\,m^{-3}$ with maximum concentrations of almost 35 $\mu g\,m^{-3}$. This period, especially from 25 to 28 May was characterized by decreasing organic and increasing nitrate contributions. In March 2009, the dominance of nitrate (42 %) and organics (22 %) contribution to the average non-refractory particulate aerosol composition (bottom panel in Fig. 1b), is interchanged compared to May 2008. Furthermore, an average mass loading of only 5.62 $\mu g\,m^{-3}$ was measured. Since westerly winds dominated during March 2009 the aerosol particles had a significantly shorter time over land and therefore a limited time to take up organic species. This fact in combination with the generally reduced biogenic activity in winter time and reduced photochemistry can explain the reduced organic contribution to the average particle composition in March 2009 compared to May 2008. The average fractional abundances of sulfate, ammonium and chloride show only minor differences between 2008 and 2009.

3.2.1 CE

The determination of the absolute mass loading in the AMS requires the knowledge of the CE. The lower panel of Fig. 3 shows the ratio of the total mass detected by the AMS to the mass derived from SMPS measurements (AMS/SMPS, black squares)

ACPD
11, 27661–27699, 2011

versus the particulate nitrate mass fraction (MF_{NO_3}). The particulate aerosol mass was determined from the measured SMPS number distributions according to the following steps. Each number distribution was transferred into a volume distribution under the assumption of spherical particles. In each measurement interval the fractional abundance of the individual species determined by the AMS was used to calculate the particle density. Densities of dry NH_4NO_3 (1.72 g cm^{-3}) and $(NH_4)_2SO_4$ (1.77 g cm^{-3}) were used as well as a density of 1.40 g cm^{-3} for organics (Hallquist et al., 2009). The chloride detected in the AMS needs to flash evaporate at the vaporizer temperature of about 600 °C. The probability that this chloride origins from an inorganic salt is very small. We set the density of the chloride fraction to 1.00 g cm^{-3} and expect only a minor impact on the average particle density in view of the low fractional abundance of 1 % and 3 %, respectively, in the two measurement periods. The mass was then calculated by combination of the volume and the density information. The upper panel of Fig. 3 shows the ratio of AMS nitrate to the particulate MARGA-Sizer nitrate of the 1 mm channel (AMS_{NO_3}/$MARGA_{NO_3,1.00}$) in blue and the according ratio for sulfate (AMS_{SO_4}/$MARGA_{SO_4,1.00}$) in red. In both panels an inflection of the mass ratios at a MF_{NO_3} of about 0.3 can be seen. This inflection is mass and time independent and is controlled mainly by the nitrate mass fraction. Comparisons to results of other AMS measurements performed at other locations during that campaign indicate a general behavior across Europe (D. Worsnop, personal communication, 2010). This finding further supports the known fact of a composition dependent CE of the AMS (Matthew et al., 2008; Crosier et al., 2007). Therefore, the CE applied for the two campaigns presented here takes the MF_{NO_3} dependent behavior into account. A constant CE of 0.5 was applied to all measurements with a MF_{NO_3} below 0.3 (Eq. 1a) and the CE of particles with higher nitrate fractions was calculated according to Eq. (1b):

$$CE = 0.5 \quad \text{for} \quad MF_{NO_3} < 0.3 \tag{1a}$$

$$CE = 0.26 + 0.94 \times MF_{NO_3} \quad \text{for} \quad MF_{NO_3} \geq 0.3 \tag{1b}$$

ACPD
11, 27661–27699, 2011

The change of the AMS/SMPS mass ratio after application of this CE is shown by the grey dots in the lower panel of Fig. 3 (right axis). The magnitude of the standard deviation of the AMS/SMPS ratio is reduced from 24 % to 18 % and the ratio has a value of 1.03 ± 0.18 after application of the CE to the AMS data.

In 2008 the AMS measured ammonium concentration exceeded the mass needed for neutralization of nitrate and sulfate by about 20 %. Artifacts from data analysis can be ruled out since special attention was paid in terms of possible interferences and relative ionization efficiency of ammonium determined by repeated ionization efficiency calibrations. Further characterization of the measurement location is needed for a final explanation of this observation, since a chicken farm is located only about 600 m north west of the CESAR tower. We speculate that our observed excess ammonium has agricultural sources, since high concentrations of nitrogen containing compounds such as ammonia and amines are known not only to be in the manure but to evaporate in significantly amounts (Rotz, 2004).

3.2.2 Diurnal cycles

Figure 4 shows the diurnal averages of individual aerosol components for the episodes defined above based on main meteorological conditions. In 2008 (left part of Fig. 4) nitrate showed a night time maximum if the entire measurement period is taken into account (most upper panel). While this maximum is very pronounced for the two episodes 1 May to 16 May (easterly winds, lowest left panel) and 21 May to 28 May (Sahara dust episode, second upper left panel) it is barely recognizable for the scavenged background situation (second lowest left panel). Night time maxima of nitrate not only in the fractional abundance but even in absolute mass concentration were found also at other measurement sites during the EUCAARI campaign. Likely this is due to heterogeneous N_2O_5 conversion in the night and to volatilization of (ammonium) nitrate during the day. In contrast to nitrate, sulfate is characterized by a daytime maximum during all periods of the campaign, in accordance with its photochemical formation. Even a distinct peak in sulfate concentration right before noon can be recognized during the scavenged

ACPD
11, 27661–27699, 2011

background situation. On average, organics show a slightly higher concentration during the night (most upper left panel). This night time maximum is most pronounced during the first half of May 2008 (lowest left panel). The average diurnal circle of the measurement campaign in March 2009 (most upper right panel) shows no pronounced maxima or minima in any specie. In the first measurement period from 24 February to 3 March (lowest right panel) when southerly and westerly winds dominated, diurnal cycles with a night time maximum in nitrate, a daytime maximum in sulfate but only slight diurnal variations in organics and ammonium can be found. Though the second period in 2009 from 9 March to 17 March is a low loading period similar to the scavenged background situation on 2008 the diurnal evolution of the individual species is similar to the first period. This is most probably due to the same wind situation, where origins range from south to north but only passing westerly directions. As opposed to the two periods just mentioned, the wind originated from easterly directions in the third period from 17 March to 20 March. In this case, daytime maxima are observed not only in sulfate and ammonium but also in nitrate. In general, ammonium diurnal cycles in 2008 and 2009 can be explained based on the sum contribution of ammonium to ammonium nitrate and ammonium sulfate. The diurnal cycles of nitrate, sulfate and ammonium observed during the two campaigns agree well with observations reported by Schaap et al. (2010) for PM_{10} diurnal cycles measured with MARGA.

3.2.3 Chemical size distribution

Campaign averages of chemically resolved size distributions as measured by the AMS at CESAR tower in 2008 (dashed lines) and 2009 (solid lines) are shown in Fig. 5. Before averaging, a boxcar smooth (box width = 3) was performed on each size distribution. The mode diameter of the total mass (black line) is about 500 nm in both measurement periods. The inorganic species are predominately detected in the larger size fraction while organic show a much broader size distribution extending into size fractions below 100 nm. Main differences between the two observation periods are the larger modal size of nitrate in 2008 than 2009 and the larger fraction of organics

ACPD
11, 27661–27699, 2011

that is observed at small sizes in 2009 compared to 2008. On average 30 % of the observed organics are due to particles with diameters below 200 nm in March 2009. In comparison only 20 % of the organics are found in the size range below 200 nm in May 2008.

3.3 Comparisons

3.3.1 SMPS

A Scanning Mobility Particle Sizer (SMPS TSI 3034) attached to the same sampling line as the AMS was operated by TNO from 14 May 2008 to End of May 2008. The time series of the mass loading derived from these SMPS measurements (red) and the total particulate mass loading of the AMS (black) is shown in Fig. 6. The measurements show very good quantitative and qualitative agreement, since even small temporal loading variations are visible in both time series. Correlating the SMPS derived mass to the total AMS mass results in a slope of 0.93 ($R^2 = 0.87$) even when the Sahara dust event is included. High mass loadings of more than 20 $\mu g\,m^{-3}$ were measured during the Sahara dust event.

3.3.2 MARGA

The AMS data are further compared to measurements obtained with a MARGA-Sizer, which was available in May 2008 (Fig. 7). Here, we only present the comparison to data acquired with the 560 nm sampling inlet of the MARGA-Sizer. Figure 7 is separated into four panels presenting from top to bottom the particulate chloride (Cl), ammonium (NH_4), sulfate (SO_4) and nitrate (NO_3) concentrations measured by AMS (colored lines) and MARGA-Sizer (black lines). The respective time series follow each other very well and very good quantitative agreement is achieved. Since the AMS is a PM_1 instrument best quantitative agreement was expected with the data obtained through the 1.00 µm channel. However, the measurement results of the 1.00 µm MARGA-sizer channel are

ACPD
11, 27661–27699, 2011

on average a factor of two higher than the AMS results, which is in the range of the scaling factor of 1.8 applied to the MARGA-Sizer data equivalence with the standard MARGA-2S. Correlations of the individual species for AMS and the 560 nm channel of the MARGA-Sizer show ratios ranging from 0.79 and 0.84 for ammonium and chloride, respectively, to 1.18 and 1.16 for nitrate and sulfate, respectively. It should be noted that even though the quantitative agreement of AMS and MARGA-Sizer was best for the 560 nm channel, the coefficients of determination (R^2) were higher for the comparison of AMS with the 1 µm channel (see Table 1). This indicates that indeed the variation of the concentrations observed by the AMS was better fetched by the 1 µm channel. The difference in absolute mass concentration between the AMS and the 1 µm channel of the MARGA-Sizer could be due to different sample positions for the AMS (60 m) and MARGA-Sizer (4 m), since the observed mass will depend on the vertical distribution of species as well as on the losses within the sampling line. Considering the instrumental accuracies and limitations due to different sampling locations AMS and MARGA-Sizer show good agreement.

3.3.3 TD-PTR-MS

During May 2008, the TD-PTR-MS was applied for measurements of individual components in the PM_2 range. The single highest signal was detected at *m/z* 46, which is attributed to NO_2^+. Note that unambiguous ion composition assignment is hindered here by the use of a Quadrupole MS. Concentrations were calculated using a molecular weight of 62 g mole^{-1} (NO_3) and a default reaction rate constant for proton transfer of 0.85×10^{-9} cm^3 s^{-1} molecule^{-1}. The detection of ammonium nitrate and the accuracy of the parameters were confirmed in laboratory experiments. Figure 8 (lower panel) shows that the TD-PTR-MS derived nitrate corresponds quite well to the AMS nitrate ($R^2 = 0.59$). It is interesting to note that the built-up of high night time concentrations in the period 9–13 May was not observed with the TD-PTR-MS. The reason for this is not known at this point. The middle panel in Fig. 8 compares the total organic signal measured with the TD-PTR-MS (all aerosol species except *m/z* 46) and the particulate

ACPD
11, 27661–27699, 2011

organic fraction detected in the AMS. In the period 9 May to 16 May the TD-PTR-MS total organic signal was about 30 % of the AMS organic concentration. This fraction is lower than previously published values of comparisons to other AMS measurements, however, in the period 17 May to 20 May the TD-PTR-MS total organic signal was about 85 % of AMS organic concentration. During this period very clean conditions prevailed and the high fraction detected with the TD-PTR-MS is in agreement with data from the Mt. Sonnblick observatory (Holzinger et al., 2010a). A relatively high correlation of the TD-PTR-MS signal at *m/z* 149 with AMS chloride is achieved in the time from 15 May midnight to 17 May midnight ($R^2 = 0.76$) as shown in Fig. 9 (lower panel). This time period includes a distinct peak in chloride concentration that was not only captured by AMS and TD-PTR-MS but also by the water soluble chloride detecting MARGA-Sizer (compare top panel in Fig. 7). The ratio of signals detected at *m/z* 149, *m/z* 150 and *m/z* 151 suggests that organic species with one chloride atom such as $C_6H_9ClO_2$ could cause the majority of the signal. However, since the TD-PTR-MS was operated with a Quadrupole MS, we cannot exclude the contribution of several other species to the signal detected at *m/z* 149. Utilizing the high resolution capabilities of the AMS, we could identify a mass peak at *m/z* 148.029 ($C_6H_9ClO_2$) that is indicative of an organic chloride source (red line in upper panel of Fig. 9). Together the possible organic sources of chloride determined by the AMS and the TD-PTR-MS results supports the expectation that AMS chloride originates from organic compounds as discussed earlier.

4 Summary and conclusion

Extensive aerosol chemical composition measurements over the course of several weeks were performed at the CESAR tower, The Netherlands, in May 2008 and March 2009. While the measurement period in 2008 was dominated by organics (40 %), nitrate was the dominant specie detected in 2009 (42 %). In both years, nitrate was the most abundant inorganic specie detected in AMS and MARGA measurements. The phenomenon of high nitrate fractional abundances is not only typical for

ACPD
11, 27661–27699, 2011

the measurement location (ten Brink et al., 2009) but is known to occur all over Europe (ten Brink et al., 1997; Putaud et al., 2004). For the first time, a nitrate dependent CE was applied for quantifying AMS data. The CE increased linearly for particulate nitrate fractions exceeding 0.3. A possible explanation is the reduced tendency of particles bouncing at elevated nitrate content. This parameterization seems to be valid for all Central European measurement locations during the EUCAARI measurement campaign (D. Worsnop, personal communication, 2010). The average aerosol particulate mass loading was 9.72 $\mu g\,m^{-3}$ in 2008 and 5.62 $\mu g\,m^{-3}$ in 2009, which is in good agreement with $PM_{2.5}$ concentrations determined at different rural European locations (Van Dingenen et al., 2004).

Size resolved mass distribution measurements of the individual species detected in the AMS indicate a mode diameter at 400 nm to 500 nm for the total mass as well as for the inorganic species. The mass distribution of organics is much broader and extents into the size range below 100 nm. Similar size distributions with inorganic species dominating in the larger size fraction and a bimodal behavior of organics have often been observed in AMS measurements independent of location (Alfarra et al., 2004; Allan et al., 2003).

Comparison of AMS total mass to the mass derived from SMPS measurements show high qualitative and quantitative agreement. In 2008 a MARGA-Sizer was operated at CESAR tower and comparison of the various inlet channels to AMS data show best correlation for the 1 µm channel. However, the mass concentrations of this channel were on average a factor of 2 higher than the AMS total mass loading. Best quantitative agreement between AMS and MARGA-Sizer was obtained through the $PM_{0.56}$ channel. Since this data present the first comparison of AMS and MARGA-Sizer of ambient aerosol particles, further parallel sampling campaigns are needed to investigate the presented discrepancy. For the first time, a comparison of AMS data to data obtained with the newly developed TD-PTR-MS is performed. Surprisingly, best qualitative and quantitative agreement was achieved for the particulate nitrate concentration, which is dominantly of inorganic origin. The total organic mass detected by the TD-PTR-

ACPD
11, 27661–27699, 2011

MS accounted for 30 % to 85 % of the organic mass detected by the AMS depending on the measurement period. Further intensive parallel measurements are needed in the future for a deeper understanding of differences in detected mass and temporal evolution.

Acknowledgement. This work was supported through the FP6 project EUCAARI (Contract 34684) and EUSAAR (European Supersites for Atmospheric Aerosol Research, EU FP6 Integrated Infrastructures Initiatives project, No. FP6-026140).

We appreciate the support from KNMI in hosting the experiment at Cabauw and for the access to meteorological data from the tower. The authors thank the CESAR tower team, especially Marcel Brinkenberg and Jaques Warmer for the big support during both campaigns. Further thanks go to P. Jongejan for his effort in operating both MARGA's.

References

Aiken, A. C., Salcedo, D., Cubison, M. J., Huffman, J. A., DeCarlo, P. F., Ulbrich, I. M., Docherty, K. S., Sueper, D., Kimmel, J. R., Worsnop, D. R., Trimborn, A., Northway, M., Stone, E. A., Schauer, J. J., Volkamer, R. M., Fortner, E., de Foy, B., Wang, J., Laskin, A., Shutthanandan, V., Zheng, J., Zhang, R., Gaffney, J., Marley, N. A., Paredes-Miranda, G., Arnott, W. P., Molina, L. T., Sosa, G., and Jimenez, J. L.: Mexico City aerosol analysis during MILAGRO using high resolution aerosol mass spectrometry at the urban supersite (T0) – Part 1: Fine particle composition and organic source apportionment, Atmos. Chem. Phys., 9, 6633–6653, doi:10.5194/acp-9-6633-2009, 2009.

ten Brink, H., Kruisz, C., Kos, G. P. A., and Berner, A.: Composition/size of the light-scattering aerosol in the Netherlands, Atmos. Environ., 31, 3955–3962, 1997.

ten Brink, H., Otjes, R., Jongejan, P., and Slanina, S.: An instrument for semi-continuous monitoring of the size-distribution of nitrate, ammonium, sulphate and chloride in aerosol, Atmos. Environ., 41, 2768–2779, 2007.

ten Brink, H., Otjes, R., Jongejan, P., and Kos, G.: Monitoring of the ratio of nitrate to sulphate in size-segregated submicron aerosol in the Netherlands, Atmos. Res, 92, 270–276, 2009.

ACPD

11, 27661–27699, 2011

Canagaratna, M. R., Jayne, J. T., Jimenez, J. L., Allan, J. D., Alfarra, M. R., Zhang, Q., Onasch, T. B., Drewnick, F., Coe, H., Middlebrook, A., Delia, A., Williams, L. R., Trimborn, A. M., Northway, M. J., DeCarlo, P. F., Kolb, C. E., Davidovits, P., and Worsnop, D. R.: Chemical and microphysical characterization of ambient aerosols with the aerodyne aerosol mass spectrometer, Mass Spectrom. Rev., 26, 185–222, 2007.

Crosier, J., Allan, J. D., Coe, H., Bower, K. N., Formenti, P., and Williams, P. I.: Chemical composition of summertime aerosol in the Po Valley (Italy), Northern Adriatic and Black Sea, Q. J. Roy. Meteor. Soc., 133, 61–75, 2007.

DeCarlo, P. F., Kimmel, J. R., Trimborn, A., Northway, M. J., Jayne, J. T., Aiken, A. C., Gonin, M., Fuhrer, K., Horvath, T., Docherty, K. S., Worsnop, D. R., and Jimenez, J. L.: Field-deployable, high-resolution, time-of-flight aerosol mass spectrometer, Anal. Chem., 78, 8281–8289, 2006.

Dentener, F. J. and Crutzen, P. J.: Reaction of N_2O_5 on tropospheric aerosols: impact on the global distributions of NO_x, O_3, and OH, J. Geophys. Res., 98, 7149–7163, doi:10.1029/92jd02979, 1993.

Drewnick, F., Schwab, J. J., Jayne, J. T., Canagaratna, M., Worsnop, D. R., and Demerjian, K. L.: Measurement of ambient aerosol composition during the PMTACS-NY 2001 using an aerosol mass spectrometer. Part I: Mass concentrations, Aerosol Sci. Tech., 38, 92–103, 2004.

Hallquist, M., Wenger, J. C., Baltensperger, U., Rudich, Y., Simpson, D., Claeys, M., Dommen, J., Donahue, N. M., George, C., Goldstein, A. H., Hamilton, J. F., Herrmann, H., Hoffmann, T., Iinuma, Y., Jang, M., Jenkin, M. E., Jimenez, J. L., Kiendler-Scharr, A., Maenhaut, W., McFiggans, G., Mentel, Th. F., Monod, A., Prévôt, A. S. H., Seinfeld, J. H., Surratt, J. D., Szmigielski, R., and Wildt, J.: The formation, properties and impact of secondary organic aerosol: current and emerging issues, Atmos. Chem. Phys., 9, 5155–5236, doi:10.5194/acp-9-5155-2009, 2009.

Hamburger, T., McMeeking, G., Minikin, A., Birmili, W., Dall'Osto, M., O'Dowd, C., Flentje, H., Henzing, B., Junninen, H., Kristensson, A., de Leeuw, G., Stohl, A., Burkhart, J. F., Coe, H., Krejci, R., and Petzold, A.: Overview of the synoptic and pollution situation over Europe during the EUCAARI-LONGREX field campaign, Atmos. Chem. Phys., 11, 1065–1082, doi:10.5194/acp-11-1065-2011, 2011.

Hansel, A., Jordan, A., Holzinger, R., Prazeller, P., Vogel, W., and Lindinger, W.: Proton-transfer reaction mass-spectrometry – online trace gas-analysis at the Ppb level, Int. J. Mass Spectrom., 150, 609–619, 1995.

ACPD
11, 27661–27699, 2011

Holzinger, R., Kasper-Giebl, A., Staudinger, M., Schauer, G., and Röckmann, T.: Analysis of the chemical composition of organic aerosol at the Mt. Sonnblick observatory using a novel high mass resolution thermal-desorption proton-transfer-reaction mass-spectrometer (hr-TD-PTR-MS), Atmos. Chem. Phys., 10, 10111–10128, doi:10.5194/acp-10-10111-2010, 2010a.

Holzinger, R., Williams, J., Herrmann, F., Lelieveld, J., Donahue, N. M., and Röckmann, T.: Aerosol analysis using a Thermal-Desorption Proton-Transfer-Reaction Mass Spectrometer (TD-PTR-MS): a new approach to study processing of organic aerosols, Atmos. Chem. Phys., 10, 2257–2267, doi:10.5194/acp-10-2257-2010, 2010b.

Huffman, J. A., Jayne, J. T., Drewnick, F., Aiken, A. C., Onasch, T., Worsnop, D. R., and Jimenez, J. L.: Design, modeling, optimization, and experimental tests of a particle beam width probe for the aerodyne aerosol mass spectrometer, Aerosol Sci. Tech., 39, 1143–1163, 2005.

IPCC: Intergovernmental Panel on Climate Change: Climate Change 2007: The Physical Science Basis, Cambrige University Press, 2007.

Jayne, J. T., Leard, D. C., Zhang, X. F., Davidovits, P., Smith, K. A., Kolb, C. E., and Worsnop, D. R.: Development of an aerosol mass spectrometer for size and composition analysis of submicron particles, Aerosol Sci. Tech., 33, 49–70, 2000.

Jimenez, J. L., Jayne, J. T., Shi, Q., Kolb, C. E., Worsnop, D. R., Yourshaw, I., Seinfeld, J. H., Flagan, R. C., Zhang, X. F., Smith, K. A., Morris, J. W., and Davidovits, P.: Ambient aerosol sampling using the aerodyne aerosol mass spectrometer, J. Geophys. Res.-Atmos., 108, 8425, doi:10.1029/2001JD001213, 2003.

Jimenez, J. L., Canagaratna, M. R., Donahue, N. M., Prevot, A. S. H., Zhang, Q., Kroll, J. H., DeCarlo, P. F., Allan, J. D., Coe, H., Ng, N. L., Aiken, A. C., Docherty, K. S., Ulbrich, I. M., Grieshop, A. P., Robinson, A. L., Duplissy, J., Smith, J. D., Wilson, K. R., Lanz, V. A., Hueglin, C., Sun, Y. L., Tian, J., Laaksonen, A., Raatikainen, T., Rautiainen, J., Vaattovaara, P., Ehn, M., Kulmala, M., Tomlinson, J. M., Collins, D. R., Cubison, M. J., E., Dunlea, J., Huffman, J. A., Onasch, T. B., Alfarra, M. R., Williams, P. I., Bower, K., Kondo, Y., Schneider, J., Drewnick, F., Borrmann, S., Weimer, S., Demerjian, K., Salcedo, D., Cottrell, L., Griffin, R., Takami, A., Miyoshi, T., Hatakeyama, S., Shimono, A., Sun, J. Y., Zhang, Y. M., Dzepina, K., Kimmel, J. R., Sueper, D., Jayne, J. T., Herndon, S. C., Trimborn, A. M., Williams, L. R., Wood, E. C., Middlebrook, A. M., Kolb, C. E., Baltensperger, U., and Worsnop, D. R.: Evolution of organic aerosols in the atmosphere, Science, 326, 1525–

ACPD
11, 27661–27699, 2011

1529, doi:10.1126/science.1180353, 2009.
Kulmala, M., Asmi, A., Lappalainen, H. K., Carslaw, K. S., Pöschl, U., Baltensperger, U., Hov, Ø., Brenquier, J.-L., Pandis, S. N., Facchini, M. C., Hansson, H.-C., Wiedensohler, A., and O'Dowd, C. D.: Introduction: European Integrated Project on Aerosol Cloud Climate and Air Quality interactions (EUCAARI) – integrating aerosol research from nano to global scales, Atmos. Chem. Phys., 9, 2825–2841, doi:10.5194/acp-9-2825-2009, 2009.
Kulmala, M., Asmi, A., Lappalainen, H. K., Baltensperger, U., Brenguier, J.-L., Facchini, M. C., Hansson, H.-C., Hov, Ø., O'Dowd, C. D., Pöschl, U., Wiedensohler, A., Boers, R., Boucher, O., de Leeuw, G., Denier van den Gon, H., Feichter, J., Krejci, R., Laj, P., Lihavainen, H., Lohmann, U., McFiggans, G., Mentel, T., Pilinis, C., Riipinen, I., Schulz, M., Stohl, A., Swietlicki, E., Vignati, E., Amann, M., Amann, M., Alves, C., Arabas, S., Artaxo, P., Beddows, D. C. S., Bergström, R., Beukes, J. P., Bilde, M., Burkhart, J. F., Canonaco, F., Clegg, S., Coe, H., Crumeyrolle, S., D'Anna, B., Decesari, S., Gilardoni, S., Fischer, M., Fjæraa, A. M., Fountoukis, C., George, C., Gomes, L., Halloran, P., Hamburger, T., Harrison, R. M., Herrmann, H., Hoffmann, T., Hoose, C., Hu, M., Hrrak, U., Iinuma, Y., Iversen, T., Josipovic, M., Kanakidou, M., Kiendler-Scharr, A., Kirkevåg, A., Kiss, G., Klimont, Z., Kolmonen, P., Komppula, M., Kristjánsson, J.-E., Laakso, L., Laaksonen, A., Labonnote, L., Lanz, V. A., Lehtinen, K. E. J., Makkonen, R., McMeeking, G., Merikanto, J., Minikin, A., Mirme, S., Morgan, W. T., Nemitz, E., O'Donnell, D., Panwar, T. S., Pawlowska, H., Petzold, A., Pienaar, J. J., Pio, C., Plass-Duelmer, C., Prévôt, A. S. H., Pryor, S., Reddington, C. L., Roberts, G., Rosenfeld, D., Schwarz, J., Seland, Ø., Sellegri, K., Shen, X. J., Shiraiwa, M., Siebert, H., Sierau, B., Simpson, D., Sun, J. Y., Topping, D., Tunved, P., Vaattovaara, P., Vakkari, V., Veefkind, J. P., Visschedijk, A., Vuollekoski, H., Vuolo, R., Wehner, B., Wildt, J., Woodward, S., Worsnop, D. R., van Zadelhoff, G.-J., Zardini, A. A., Zhang, K., van Zyl, P. G., Kerminen, V.-M., S. Carslaw, K., and Pandis, S. N.: General overview: European Integrated project on Aerosol Cloud Climate and Air Quality interactions (EUCAARI) – integrating aerosol research from nano to global scales, Atmos. Chem. Phys. Discuss., 11, 17941–18160, doi:10.5194/acpd-11-17941-2011, 2011.
Lindinger, W., Hansel, A., and Jordan, A.: Proton-transfer-reaction mass spectrometry (PTR-MS): on-line monitoring of volatile organic compounds at pptv levels, Chem. Soc. Rev., 27, 347–354, 1998.
Liu, P., Ziemann, P. J., Kittelson, D. B., and McMurry, P. H.: Generating particle beams of controlled dimensions and divergence: I. Theory of particle motion in aerodynamic lenses

ACPD
11, 27661–27699, 2011

and nozzle expansions, Aerosol Sci. Tech., 22, 293–313, 1995a.
Liu, P., Ziemann, P. J., Kittelson, D. B., and McMurry, P. H.: Generating particle beams of controlled dimensions and divergence: II. Experimental evaluation of particle motion in aerodynamic lenses and nozzle expansions, Aerosol Sci. Tech., 22, 314–324, 1995b.
Matthew, B. M., Middlebrook, A. M., and Onasch, T. B.: Collection efficiencies in an aerodyne aerosol mass spectrometer as a function of particle phase for laboratory generated aerosols, Aerosol Sci. Tech., 42, 884–898, 2008.
Mensah, A. A., Buchholz, A., Mentel, T. F., Tillmann, R., and Kiendler-Scharr, A.: Aerosol mass spectrometric measurements of stable crystal hydrates of oxalates and inferred relative ionization efficiency of water, J. Aerosol Sci., 42, 11–19, doi:10.1016/j.jaerosci.2010.10.003, 2011.
Monks, P. S., Granier, C., Fuzzi, S., Stohl, A., Williams, M. L., Akimoto, H., Amann, M., Baklanov, A., Baltensperger, U., Bey, I., Blake, N., Blake, R. S., Carslaw, K., Cooper, O. R., Dentener, F., Fowler, D., Fragkou, E., Frost, G. J., Generoso, S., Ginoux, P., Grewe, V., Guenther, A., Hansson, H. C., Henne, S., Hjorth, J., Hofzumahaus, A., Huntrieser, H., Isaksen, I. S. A., Jenkin, M. E., Kaiser, J., Kanakidou, M., Klimont, Z., Kulmala, M., Laj, P., Lawrence, M. G., Lee, J. D., Liousse, C., Maione, M., McFiggans, G., Metzger, A., Mieville, A., Moussiopoulos, N., Orlando, J. J., O'Dowd, C. D., Palmer, P. I., Parrish, D. D., Petzold, A., Platt, U., Pöschl, U., Prévôt, A. S. H., Reeves, C. E., Reimann, S., Rudich, Y., Sellegri, K., Steinbrecher, R., Simpson, D., ten Brink, H., Theloke, J., van der Werf, G. R., Vautard, R., Vestreng, V., Vlachokostas, C., and von Glasow, R.: Atmospheric composition change – global and regional air quality, Atmos. Environ., 43, 5268–5350, doi:10.1016/j.atmosenv.2009.08.021, 2009.
Moolgavkar, S. H.: Air Pollution and Mortality, New Engl. J. Med., 330, 1237–1238, 1994.
Morgan, W. T., Allan, J. D., Bower, K. N., Esselborn, M., Harris, B., Henzing, J. S., Highwood, E. J., Kiendler-Scharr, A., McMeeking, G. R., Mensah, A. A., Northway, M. J., Osborne, S., Williams, P. I., Krejci, R., and Coe, H.: Enhancement of the aerosol direct radiative effect by semi-volatile aerosol components: airborne measurements in North-Western Europe, Atmos. Chem. Phys., 10, 8151–8171, doi:10.5194/acp-10-8151-2010, 2010a.
Morgan, W. T., Allan, J. D., Bower, K. N., Highwood, E. J., Liu, D., McMeeking, G. R., Northway, M. J., Williams, P. I., Krejci, R., and Coe, H.: Airborne measurements of the spatial distribution of aerosol chemical composition across Europe and evolution of the organic fraction, Atmos. Chem. Phys., 10, 4065–4083, doi:10.5194/acp-10-4065-2010, 2010b.

ACPD
11, 27661–27699, 2011

Nazarenko, L. and Menon, S.: Varying trends in surface energy fluxes and associated climate between 1960 and 2002 based on transient climate simulations, Geophys. Res. Lett., 32, L22704, doi:10.1029/2005GL024089, 2005.
Nober, F. J., Graf, H.-F., and Rosenfeld, D.: Sensitivity of the global circulation to the suppression of precipitation by anthropogenic aerosols, Global Planet. Change, 37, 57–80, 2003.
Norris, J. R. and Wild, M.: Trends in aerosol radiative effects over Europe inferred from observed cloud cover, solar "dimming" and solar "brightening", J. Geophys. Res., 112, D08214, doi:10.1029/2006JD007794, 2007.
Phillips, V. T. J., Choularton, T. W., Blyth, A. M., and Latham, J.: The influence of aerosol concentrations on the glaciation and precipitation of a cumulus cloud, Q. J. Roy. Meteor. Soc., 128, 951–971, 2002.
Pope, C. A., Burnett, R. T., Thun, M. J., Calle, E. E., Krewski, D., Ito, K., and Thurston, G. D.: Lung cancer, cardiopulmonary mortality, and long-term exposure to fine particulate air pollution, J. Amer. Med. Assoc., 287, 1132–1141, doi:10.1001/jama.287.9.1132, 2002.
Putaud, J.-P., Raes, F., Van Dingenen, R., Brüggemann, E., Facchini, M. C., Decesari, S., Fuzzi, S., Gehrig, R., Hüglin, C., Laj, P., Lorbeer, G., Maenhaut, W., Mihalopoulos, N., Müller, K., Querol, X., Rodriguez, S., Schneider, J., Spindler, G., ten Brink, H., Tørseth, K., and Wiedensohler, A.: A European aerosol phenomenology – 2: Chemical characteristics of particulate matter at kerbside, urban, rural and background sites in Europe, Atmos. Environ., 38, 2579–2595, doi:10.1016/j.atmosenv.2004.01.041, 2004.
Ramanathan, V., Li, F., Ramana, M. V., Praveen, P. S., Kim, D., Corrigan, C. E., Nguyen, H., Stone, E. A., Schauer, J. J., Carmichael, G. R., Adhikary, B., and Yoon, S. C.: Atmospheric brown clouds: hemispherical and regional variations in long-range transport, absorption, and radiative forcing, J. Geophys. Res., 112, D22S21, doi:10.1029/2006JD008124, 2007.
Roelofs, G.-J., ten Brink, H., Kiendler-Scharr, A., de Leeuw, G., Mensah, A., Minikin, A., and Otjes, R.: Evaluation of simulated aerosol properties with the aerosol-climate model ECHAM5-HAM using observations from the IMPACT field campaign, Atmos. Chem. Phys., 10, 7709–7722, doi:10.5194/acp-10-7709-2010, 2010.
Rogge, W. F., Mazurek, M. A., Hildemann, L. M., Cass, G. R., and Simoneit, B. R. T.: Quantification of urban organic aerosols at a molecular level: identification, abundance and seasonal variation, Atmos. Environ. A-Gen., 27, 1309–1330, 1993.
Romanou, A., Liepert, B., Schmidt, G. A., Rossow, W. B., Ruedy, R. A., and Zhang, Y.: 20th century changes in surface solar irradiance in simulations and observations, Geophys. Res.

ACPD
11, 27661–27699, 2011

Lett., 34, L05713, doi:10.1029/2006GL028356, 2007.
Rotz, C. A.: Management to reduce nitrogen losses in animal production, J. Anim. Sci., 82, E119–137, 2004.
Russchenberg, H., Bosveld, F., Swart, D., ten Brink, H., de Leeuw, G., Uijlenhoet, R., Arbesser-Rastburg, B., van der Marel, H., Ligthart, L., Boers, R., and Apituley, A.: Ground-Based Atmospheric Remote Sensing in the Netherlands: European Outlook, The Institute of Electronics, Information and Communication Engineers, E88–B, IEICE Transactions on communications, doi:10.1093/ietcom/e88-b.6.2252, 2005.
Schaap, M., Otjes, R. P., and Weijers, E. P.: Illustrating the benefit of using hourly monitoring data on secondary inorganic aerosol and its precursors for model evaluation, Atmos. Chem. Phys. Discuss., 10, 12341–12370, doi:10.5194/acpd-10-12341-2010, 2010.
Slanina, J., ten Brink, H. M., Otjes, R. P., Even, A., Jongejan, P., Khlystov, A., Waijers-Ijpelaan, A., Hu, M., and Lu, Y.: The continuous analysis of nitrate and ammonium in aerosols by the steam jet aerosol collector (SJAC): extension and validation of the methodology, Atmos. Environ., 35, 2319–2330, 2001.
Tao, W. K., Li, X. W., Khain, A., Matsui, T., Lang, S., and Simpson, J.: Role of atmospheric aerosol concentration on deep convective precipitation: cloud-resolving model simulations, J. Geophys. Res., 112, D24S18, doi:10.1029/2007JD008728, 2007.
Trebs, I., Meixner, F. X., Slanina, J., Otjes, R., Jongejan, P., and Andreae, M. O.: Real-time measurements of ammonia, acidic trace gases and water-soluble inorganic aerosol species at a rural site in the Amazon Basin, Atmos. Chem. Phys., 4, 967–987, doi:10.5194/acp-4-967-2004, 2004.
Williams, B. J., Goldstein, A. H., Kreisberg, N. M., and Hering, S. V.: An in-situ instrument for speciated organic composition of atmospheric aerosols: Thermal Desorption Aerosol GC/MS-FID (TAG), Aerosol Sci. Tech., 40, 627–638, 2006.
Zhang, Q., Jimenez, J. L., Canagaratna, M. R., Allan, J. D., Coe, H., Ulbrich, I., Alfarra, M. R., Takami, A., Middlebrook, A. M., Sun, Y. L., Dzepina, K., Dunlea, E., Docherty, K., DeCarlo, P. F., Salcedo, D., Onasch, T., Jayne, J. T., Miyoshi, T., Shimono, A., Hatakeyama, S., Takegawa, N., Kondo, Y., Schneider, J., Drewnick, F., Borrmann, S., Weimer, S., Demerjian, K., Williams, P., Bower, K., Bahreini, R., Cottrell, L., Griffin, R. J., Rautiainen, J., Sun, J. Y., Zhang, Y. M., and Worsnop, D. R.: Ubiquity and dominance of oxygenated species in organic aerosols in anthropogenically-influenced Northern Hemisphere midlatitudes, Geophys. Res. Lett., 34, L13801, doi:10.1029/2007GL029979, 2007.

ACPD
11, 27661–27699, 2011

Zhang, X., Smith, K. A., Worsnop, D. R., Jimenez, J. L., Jayne, J. T., Kolb, C. E., Morris, J., and Davidovits, P.: Numerical characterization of particle beam collimation – Part II: Integrated Aerodynamic-Lens-Nozzle System, Aerosol Sci. Tech., 38, 619–638, 2004.

ACPD
11, 27661–27699, 2011

Table 1. Correlation of the 0.56 µm and the 1.00 µm channel of the MARGA-Sizer to AMS loadings of NO_3, SO_4, NH_4 and Cl. Presented are the slopes and one standard deviation of a linear regression over the entire measurement period in May 2008. The coefficient of determination (R^2) is given in parenthesis.

	NO_3	SO_4	NH_4	Cl
0.56 µm	1.18 ± 0.02 (0.73)	1.16 ± 0.03 (0.24)	0.79 ± 0.02 (0.40)	0.84 ± 0.04 (0.49)
1.00 µm	2.16 ± 0.04 (0.82)	1.67 ± 0.03 (0.69)	1.43 ± 0.02 (0.72)	1.43 ± 0.04 (0.70)

ACPD
11, 27661–27699, 2011

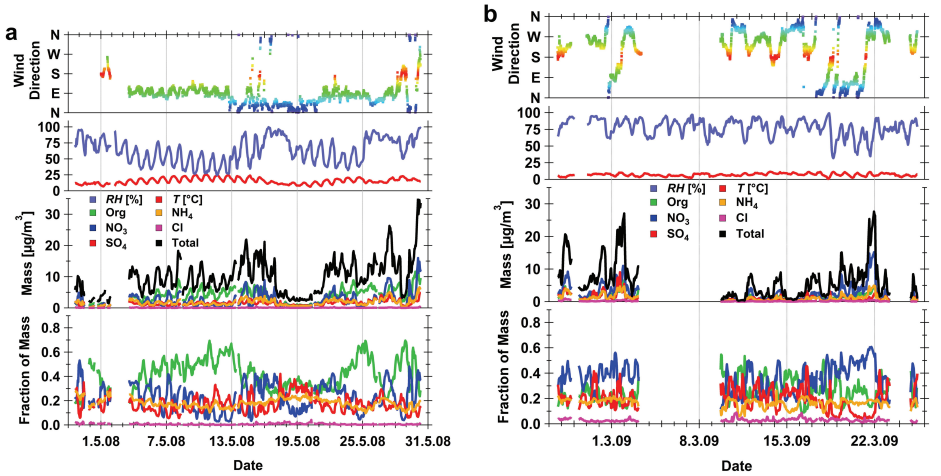

Fig. 1. Campaign overviews of aerosol chemical composition in May 2008 **(a)** and March 2009 **(b)**. Mass concentrations (second lowest panel) and relative contributions (lowest panel) are shown for total AMS measured mass (black), ammonium (orange), nitrate (blue), sulfate (red), organics (green), and chloride (purple). The ambient temperature and RH in the second upper panel as well as the wind direction in the most upper panel are given in both graphs. As a guidance of the eye, northerly wind directions are colored in blue, southerlies in red, and easterly and westerly wind directions in green.

ACPD
11, 27661–27699, 2011

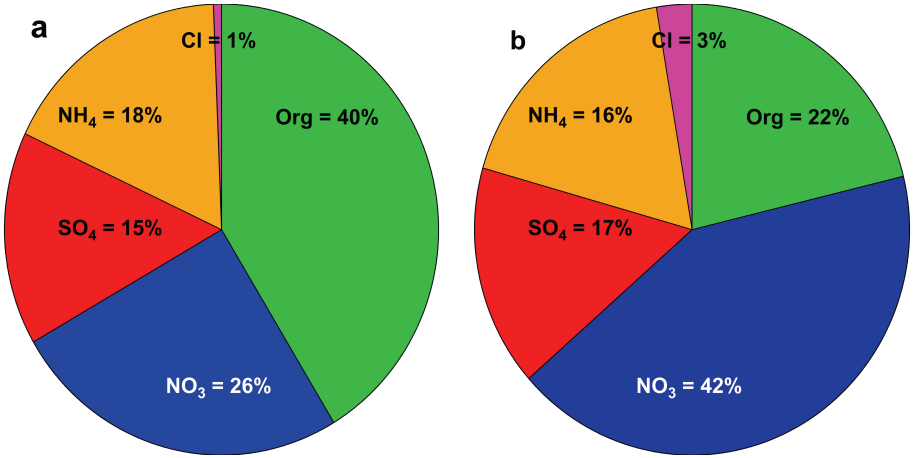

Fig. 2. Mean aerosol composition in May 2008 **(a)** and March 2009 **(b)**. While the aerosol chemical composition is dominated by organics (40 %) in May 2008, the main fraction is composed of nitrate (42 %) in March 2009.

ACPD
11, 27661–27699, 2011

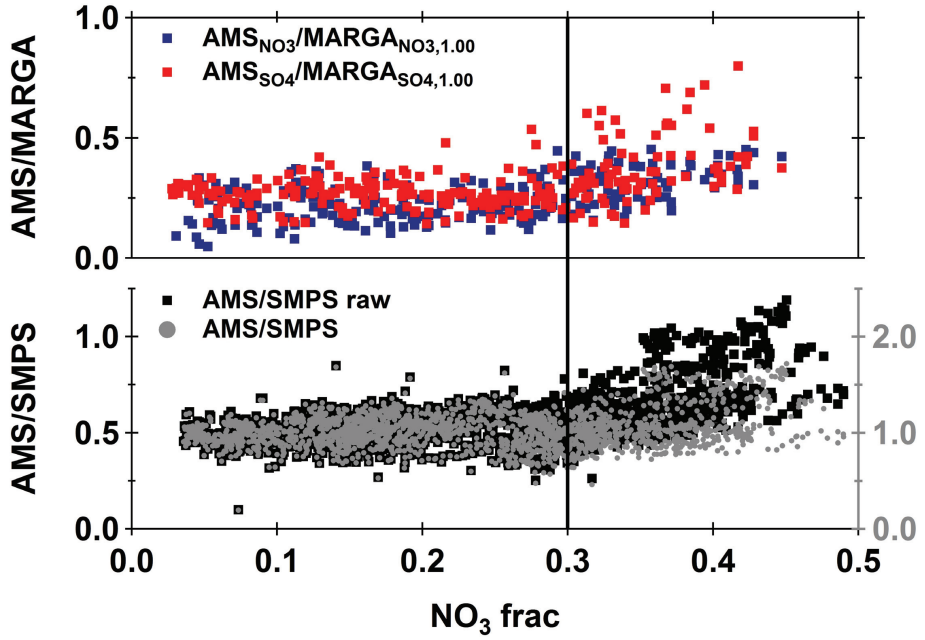

Fig. 3. Lower panel: ratio of raw (black squares, left axis) and CE corrected (grey dots, right axis) AMS total mass to SMPS derived aerosol particle mass as function of nitrate mass fraction (MF_{NO_3}) in the particles. Top panel: raw AMS/MARGA-Sizer (1.00 µm) nitrate (blue) and sulfate (red) mass ratios. Note that the CE of the AMS shows a dependence on the aerosol nitrate fraction with increasing nitrate fraction leading to increasing collection efficiency.

ACPD
11, 27661–27699, 2011

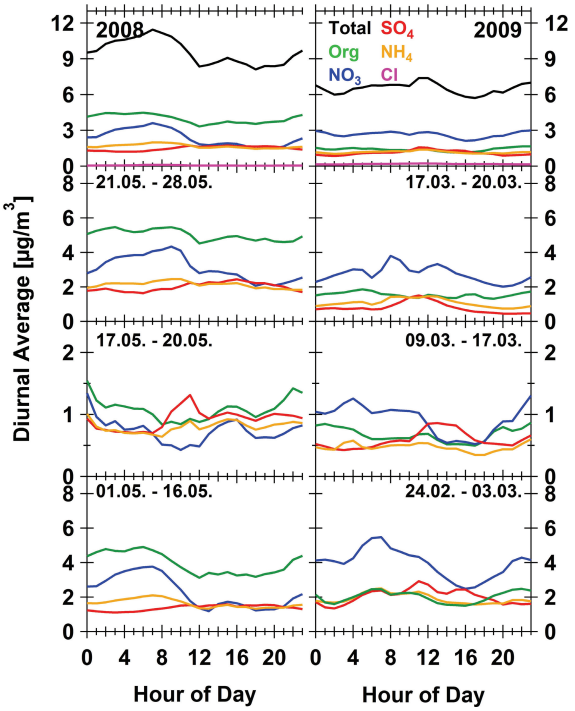

Fig. 4. Average diurnal variation of the total mass (black), organics (green), nitrate (blue), sulfate (red), ammonium (orange), and chloride (purple) as campaign averages (top panels) and for each of the individual meteorological periods encountered in May 2008 (left) and March 2009 (right).

ACPD
11, 27661–27699, 2011

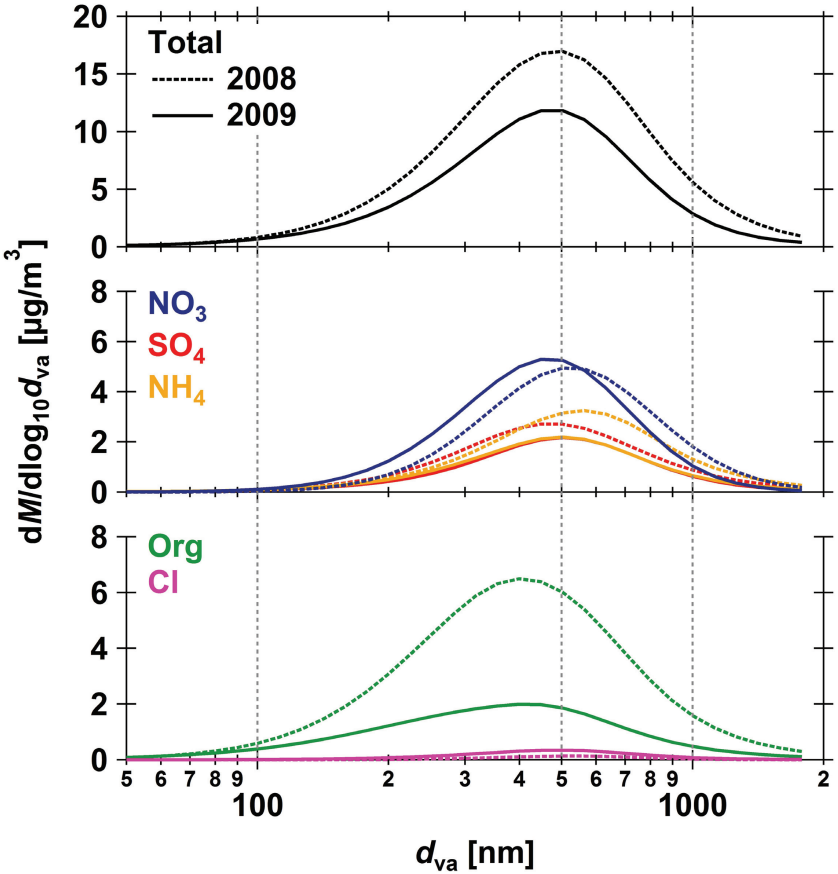

Fig. 5. Average size distribution for May 2008 (dashed lines) and March 2009 (solid lines) of the total mass (black, top panel), nitrate (blue), sulfate (red), and ammonium (orange, middle panel), and organics (green) and Chloride (purple, bottom panel).

ACPD
11, 27661–27699, 2011

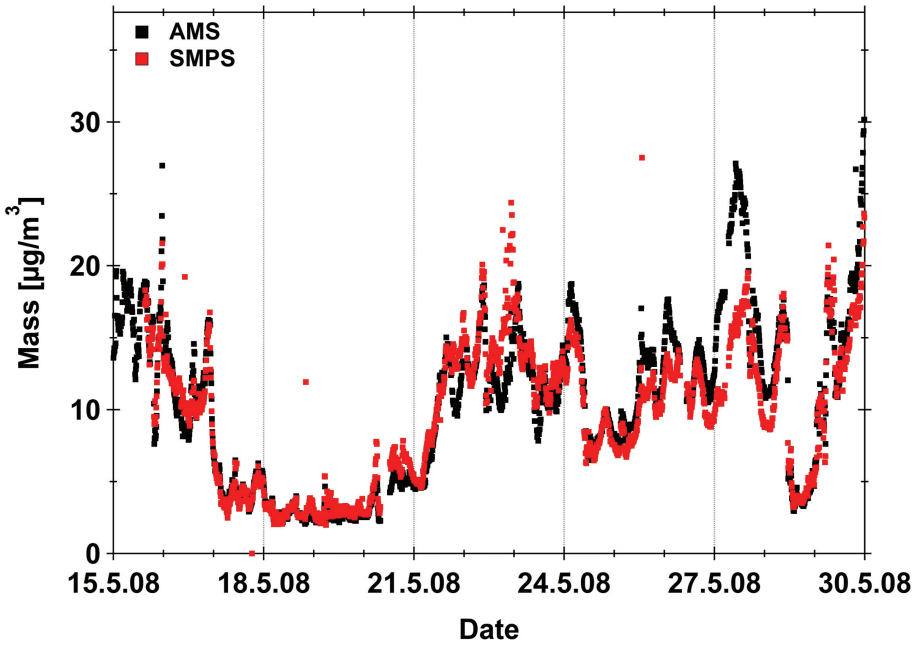

Fig. 6. Time series of AMS total mass and mass derived from SMPS measurements in 2008.

ACPD
11, 27661–27699, 2011

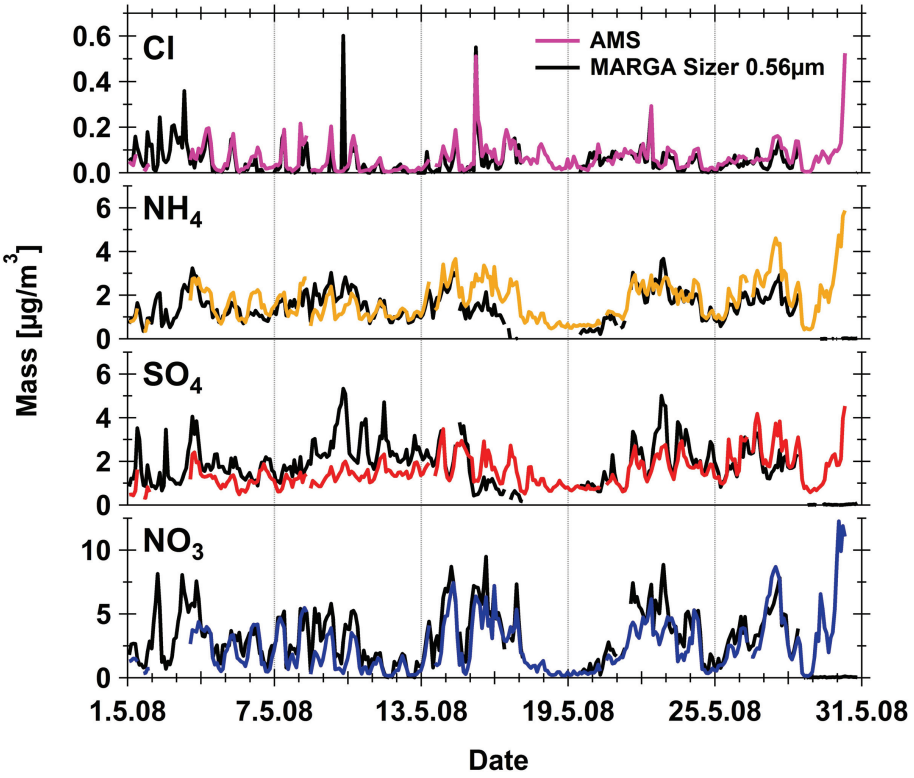

Fig. 7. Comparison of AMS chemical composition with MARGA-Sizer data for the May 2008 intensive campaign. AMS data are compared to MARGA 0.56 µm channel with good agreement in terms of both absolute mass concentration and relative trends.

ACPD
11, 27661–27699, 2011

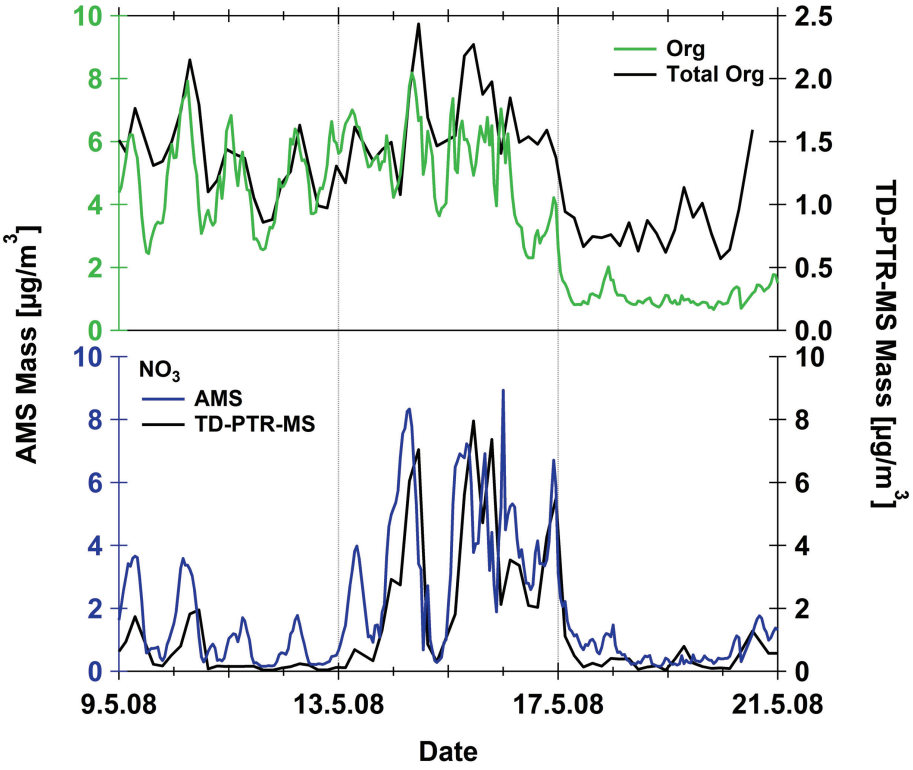

Fig. 8. Comparison of AMS to TD-PTR-MS results. Lower panel: AMS nitrate (blue, left axis) and TD-PTR-MS nitrate (*m/z* 46, black, right axis). Upper panel: AMS organic (green, left axis) and TD-PTR-MS total organic (black, right axis).

ACPD
11, 27661–27699, 2011

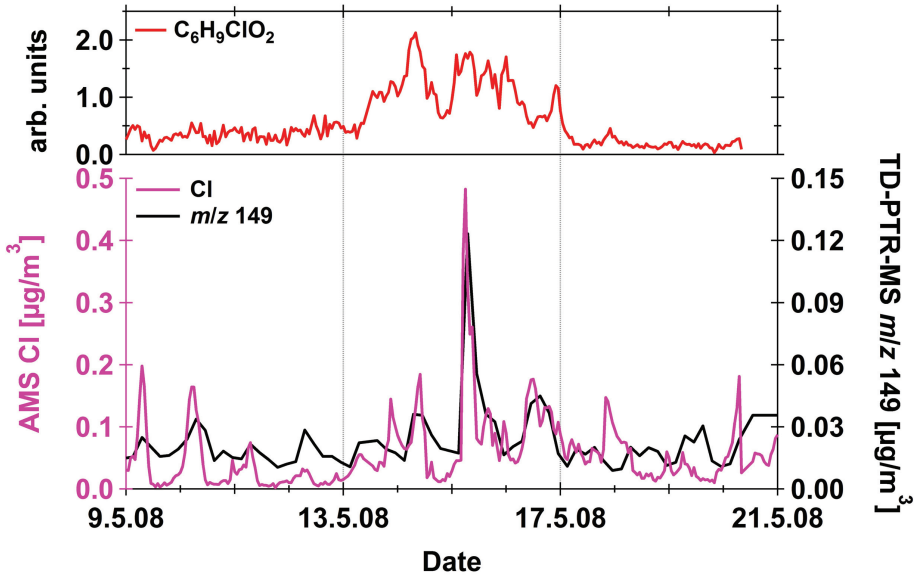

Fig. 9. Comparison of AMS to TD-PTR-MS results. Lower panel: AMS chloride (purple, left axis) and TD-PTR-MS mass trace at *m/z* 149 (black, right axis). Upper panel: AMS high resolution traces of $C_6H_9ClO_2$ (*m/z* 148.029, red).

ACPD
11, 27661–27699, 2011